1. Introduction

GTAW (Gas Tungsten Arc Welding, also known as TIG - Tungsten Inert Gas) is recognized for its high weld quality and precision, and is widely used in applications that require high thermal control and metallurgical integrity (Dutra, 2023). Despite its advantages, one of the main limitations of the conventional GTAW process is the low deposition rate when compared to processes such as GMAW (Gas Metal Arc Welding), which motivates the development of variants that combine the process quality with greater productivity (Da Cunha, dos Santos and Voigt, 2022). Among these innovations is the concept of dynamic wire feeding (TIG AD), in which the filler material is reciprocally introduced into the molten pool, resulting in improved arc stability and metal transfer efficiency (Silva, 2016)(Fronius, 2024)(EWM, 2018)(TipTIG, 2016). This approach makes it possible to combine the intrinsic thermal control of the TIG process with an increase of the deposition rate (Pigozzo et al., 2022). It is particularly promising for weld overlaying critical components. The application of orbital welding, as studied by Paes (2016), introduces new welding techniques to increase productivity for pipe welding in the oil and gas sector, demonstrating significant gains in welding speed and penetration.

Among the technological variants of the process, the TOPTIG method stands out, which integrates dynamic wire feeding at a reduced angle close to the tungsten electrode, promoting greater melting efficiency and puddle control (Silva, 2020). Studies carried out by Pigozzo (2024) investigated the advantages of dynamic feeding in the TIG process with a reduced insertion angle, focusing mainly on the metal transfer and their influence on the stability, geometry, and microstructure of the bead. Also in this study, the author developed a procedure synchronizing the moment when the wire makes contact with the weld pool to the elevation of the current until the droplet has separated from the wire. This approach allowed for lower current to be used to maintain the weld pool until the next pulse is administered, possibly reducing overlay material dilution (Pigozzo, Silva and Viviani, 2024).

These improvements are particularly relevant for surface cladding applications with high-performance alloys, such as Inconel 625 (NiCrMo-3), in which controlling the heat input and minimizing dilution are critical factors for ensuring resistance to corrosion and wear in aggressive environments (Riffel et al., 2020).

Continuing previous researches, this work aims to deepen the analysis of metal transfer mechanisms and their effects on the microstructure and stability of the process, with a focus on the application of dynamic wire feeding for cladding on low alloy steel pipes with Inconel 625.

In this context, comparative tests were carried out between three different conditions: constant current with conventional wire feed (CWF-GTAW), constant current with dynamic wire feed (DWF-GTAW) and synchronized current with dynamic wire feed (SWF-GTAW). Thus, this study aims to provide technical support for the selection and optimization of GTAW cladding processes with dynamic wire feeding, contributing to the development of industrial solutions, aligning technological and operational innovation.

2. Methodology

Experimental tests were carried out to parameterize and optimize the electrical variables, such as base and pulse welding current values, as well as the movement parameters for the TIG welding process with Dynamic Wire Feed (DWF), pursuing greater applicability to pipeline overlays with Ni alloy. Finally, the test samples were cladded. They consisted of 8 overlapping weld beads deposited along the longitudinal direction in ASTM A204 Grade B pipes. The offset (angular displacement) between each bead was 15° relative to the center of the pipe. These tests compared three variants of the TIG process: CWF-GTAW, DWF-GTAW, and SWF-GTAW. The filler material used was a Ni-based alloy, commercially known as Inconel 625 (ER NiCrMo-3), supplied as wire with diameter of 1.14 mm. The wire was fed continuously, either dynamically or synchronized with the current pulses, as

required. The optimized parameters for the proposed steel pipe cladding method incorporate internal cooling. This causes higher heat exchange between the welded pipe and the internal fluid, as in heat exchanger operating conditions, even enabling continuous welding operations. The experimental bench used for the tests is shown in Figure 1.



Figure 1. TIG AD process test bench with current synchronization and dynamic wire feed.

The welding parameters used in the test for each process variant are listed in Table 1:

Process	Current	Wire Feed	Synchronization	Torch Oscillation
CWF- GTAW	140 A (constant)	Conventional (continuous)	-	
DWF- GTAW	140 A (constant)	Dynamic (7.0 Hz)	-	Sinusoidal 6mm / 1.1Hz
SWF- GTAW	100 A (base) 160 A (pulse)	Dynamic (7.0 Hz)	Current-pulse synchronized	

Table 1. Welding parameters for CWF-GTAW, DWF-GTAW and SWF-GTAW processes.

The optical emission spectroscopy (OES) technique was used to compare the iron content on the surface of the overlays produced by the three processes. The equipment used for this analysis was a Ametek SpectroTest TXC35 portable spectrometer. This measurement is critical for applications where corrosion resistance and the integrity of the deposited material are essential. The conventional TIG process was selected for detailed analysis due to its broad industrial applicability and excellent finishing capability.

The samples were subjected to metallographic testing. They were cut crosswise, grinded, polished and electrolytic etched with Oxalic Acid reagent. Metallographic preparation revealed the microstructures of the fused and thermally affected zones, allowing for macro and optical-microscope panoramic analysis of the welds. Panoramic microscope images were taken of the overlay areas. The images consisted of: the first bead (beginning of the coating); the region between the first and second beads; the region between the 4th and 5th bead (middle of the overlay). This study was supported by chemical analysis, which helped identify certain elements present in the structure.

The hardness of the steel pipe cladded with Ni alloy wire was also evaluated. Hardness measurements of the samples cross-sections were performed using a Wilson VH1102 microhardness testing machine. The hardness profiles were measured from the surface to the base metal, with an applied load of 1 kgf and a dwell time of 10 s. As the overlay consisted of a layer of overlapping beads, different regions of the cladded material were evaluated with the hardness profile. Therefore, lines of indentation were made on each sample on the first bead of the layer (on the right), between beads 4 and 5 (in the middle) and on the eighth and last bead of the layer (on the left). The identification lines were made radially around the circumference of the pipe, as illustrated over the macrograph in Figure 2.

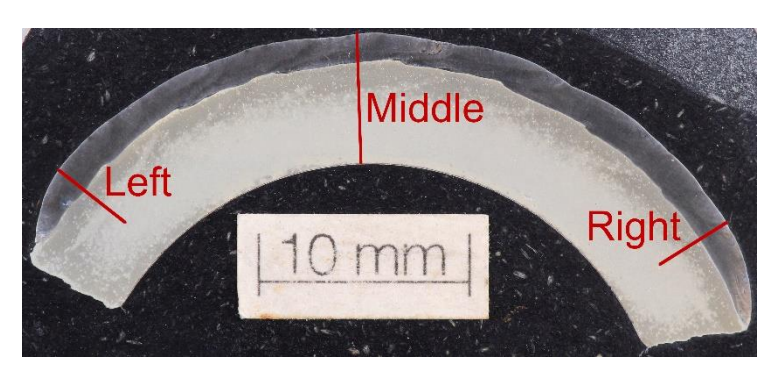


Figure 2. Macrograph showing the positioning pattern of the indentations for the microhardness tests.

3. Results and Discussions

3.1. Optical Emission Spectroscopy Analysis

The optical emission spectroscopy tests carried out on the overlays applied by the constant current with conventional wire feeding (CWF-GTAW), constant current with dynamic feed (DWF-GTAW) and pulsed current with synchronized dynamic feeding (SWF-GTAW) TIG processes revealed significant data on the dilution of the base material in the deposited material. Table 2 shows the results obtained for each process. The dilution is calculated based on the iron (Fe) content of the steel pipe (\approx 99%) and of the filler metal (\approx 0.5%) compared with the measured surface Fe% content. Equation 1 demonstrates the dilution formula. Because of the great difference of Fe content between the steel pipe and the filler metal, the dilution value should be very close to the measured surface Fe content.

Process	Fe%	Ni%	Dilution
CWF- GTAW	7.01	61.1	6.6%
DWF- GTAW	12.71	58.1	12.4%
SWF- GTAW	11.48	58.8	11.2%

Table 2. Spectroscopy results for the samples.

$$Dilution (\%) = \frac{Fe\%_{overlay} \cdot Fe\%_{wire}}{Fe\%_{tube} \cdot Fe\%_{wire}} \cdot 100$$
 (Equation 1).

The results revealed similar iron and nickel contents between the DWF and SWF processes, with nearly identical chemical compositions in the analyzed zones. Therefore, in terms of chemical composition, both processes proved technically viable for industrial applications requiring high corrosion and wear resistance. In contrast, the CWF process showed a significantly lower surface iron content, along with a slight increase in nickel content. This behavior is probably attributed to the formation of a thicker layer in this process.

3.2. Macrographic and optical-microscope panoramic analysis of the samples

3.2.1. Macrographs of the CWF-GTAW, DWF-GTAW and SWF-GTAW overlays

Macrographs of the cross-sections of the overlays obtained by the SWF-GTAW, DWF-GTAW and CWF-GTAW processes are shown in Figure 3.

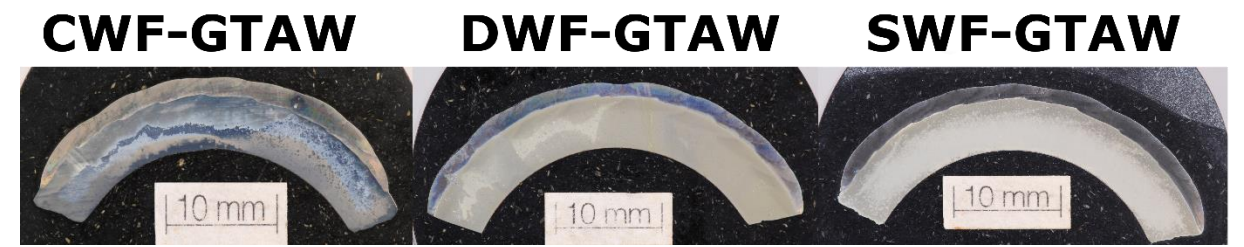


Figure 3. Comparative macrographs of the coatings applied by the CWG-GTAW, DWF-GTAW and SWF-GTAW processes.

Analysis of these images revealed that the DWF-GTAW and SWF-GTAW processes resulted in homogeneous layers with an average thickness of approximately 1.5 mm, while the CWF-GTAW process resulted in a layer approximately 2 mm thick. All overlays showed good metallurgical continuity between passes, with no evidence of typical defects such as lack of fusion or other discontinuities. The SWF-GTAW process was slightly superior in terms of bead uniformity and metallurgical continuity between the overlays; however, the difference was not significant enough to characterize a decisive

technical advantage over the DWF-GTAW process. Thus, both processes showed satisfactory performance, reinforcing the technical viability of both the dynamically fed and conventional processes for cladding applications.

3.2.2. Optical-microscope panoramic of the CWF-GTAW, DWF-GTAW and SWF-GTAW processes

Microscope panoramic of the overlay zones obtained by the CWF-GTAW, DWF-GTAW and SWF-GTAW processes are shown in Figures 4, 5 and 6.

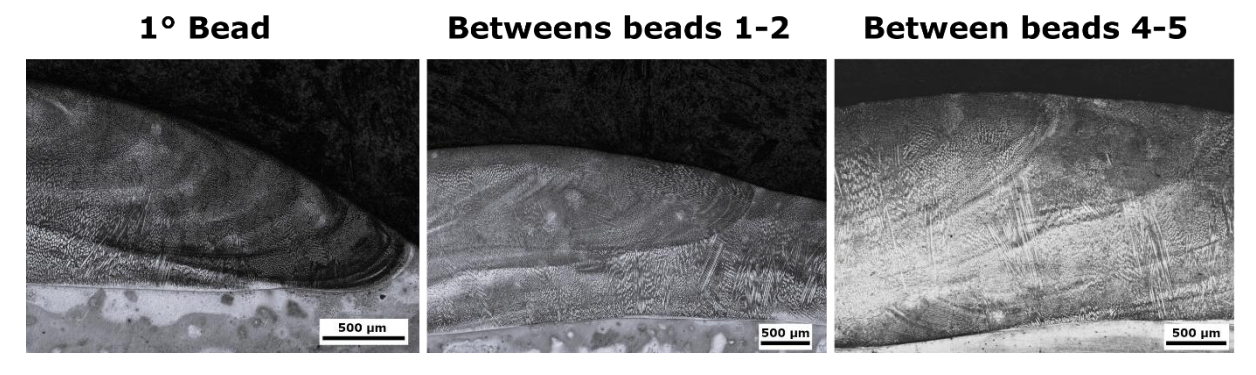


Figure 4. Optical-microscope panoramic of the inter-bead region of the process CWF-GTAW.

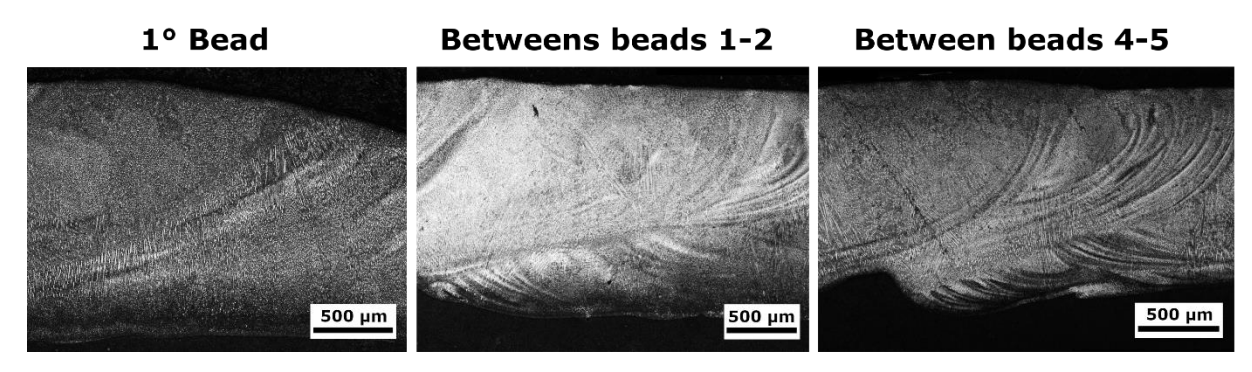


Figure 5. Optical-microscope panoramic of the inter-bead region of the process DWF-GTAW.

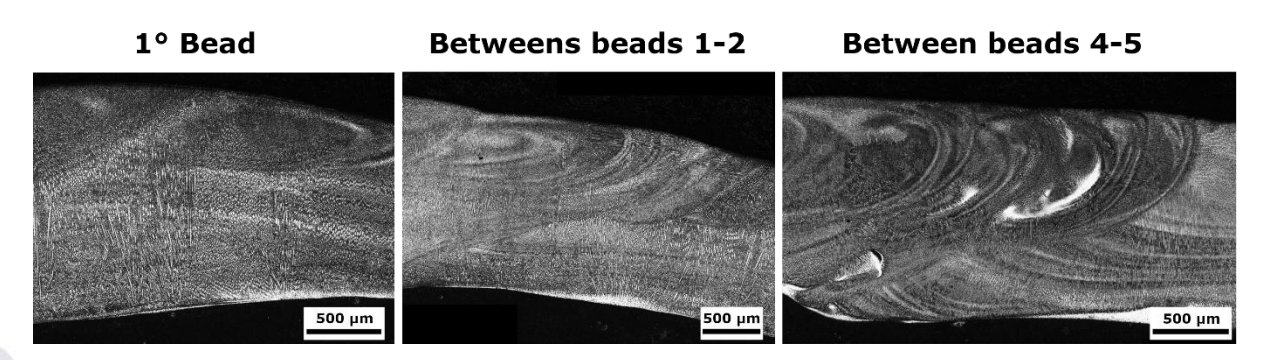


Figure 6. Optical-microscope panoramic of the inter-bead region of the process SWF-GTAW.

The images revealed greater metallurgical details of each process. The SWF-GTAW process showed signs of possible greater turbulence during solidification, hypothesized due to dynamic feeding and pulsed synchronized welding current. Both features force more molten puddle oscillation, which can cause the extra solidification fronts seen in the weld metal in Figure 6. There is also accelerated cooling due to the base period at low current levels, when compared to the other processes, which probably contributes to this metallurgy. Another possible evidence of these phenomena is the presence of regions with higher iron content, indicated in the SEM analysis, as white regions both close to the base metal and close to the bead face. These characteristics are evident in the panorama shown in Figure 6.

While the macrographs have shown better homogeneity for the overlay surface for the SWF-GTAW variant, the microscopical panoramic clearly points out the differences between this and DWF-GTAW variant, reinforcing the importance of this type of analysis.

The DWF-GTAW process showed a more homogeneous layer, with less evidence of regions with high iron content, which contributes to maintaining the properties of the deposited Inconel 625. This aspect is probably responsible for the higher surface iron content measured for this process when compared to the SWF-GTAW. Future tests may be necessary to confirm this hypothesis, but is an indication of the synchronized current potential for lowering dilution levels.

The CWF-GTAW process, on the other hand, despite a thicker layer, showed a microstructure similar to that of DWF-GTAW, but with greater variation in the thickness of the deposited layer. This may occur due to the absence of dynamic feed control, although without significantly affecting the overall quality of the overlay. These differences, although subtle, are relevant for critical applications, such as process steam and fume extraction, with higher temperatures involved, the need for thinner overlays may be a critical factor for the CWF-GTAW applicability.

3.2.3. Vickers microhardness profile

To evaluate the hardness performance of the overlays, Vickers microhardness tests were carried out on the different regions of the samples, as described in section 2. The hardness profile curves for the SWF-GTAW, DWF-GTAW and CWF-GTAW processes are shown in Figure 7.

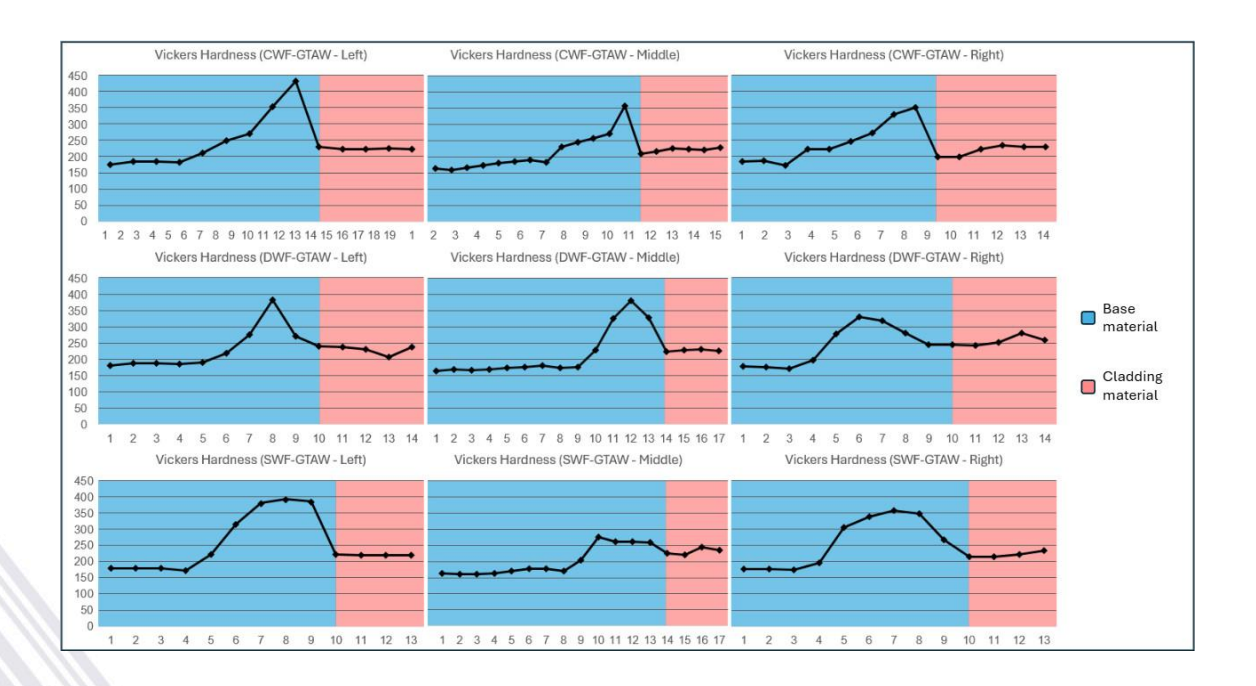


Figure 7. Hardness profile curves on the left, middle, and right of the overlays, for CWF-GTAW, DWF-GTAW and SWF-GTAW processes.

In the SWF-GTAW process (Figure 7, botton), an increase in hardness was observed from the base material (~200 HV) to the added material (~250 HV), with a hardness peak located in the coarse-grained Heat Affected Zone (HAZ CG), indicating good mechanical strength, but with controlled variation. The smoother hardness curves for this process may also be beneficial for severe operating conditions, specially for crack prevention and improved fatigue resistance. This is corroborated by the study of Trindade et al. (2017), who discuss that for coating applications on pipe walls operating continuously under dynamic loading conditions, and therefore subject to fatigue phenomena, an abrupt variation in hardness in the substrate HAZ is not desirable. Such abrupt changes in properties over a short distance favor contact fatigue, which can promote the detachment of the Inconel layer.

The DWF-GTAW process (Figure 7, middle) showed hardness profiles with greater dispersion, with sharper peaks close to 400 HV in the HAZ CG and more heterogeneous behavior in the cladded material. This behavior indicates potential fragilization, resulting from the high thermal input and fast cooling promoted by the internal cooling of the pipes.

On the other hand, the CWF-GTAW process (Figure 7, top) also showed high hardness peaks, even exceeding 400 HV. Despite this, it still showed a certain hardness constancy throughout the overlay. Variability in hardness results can be critical in certain applications, depending on the mechanical stress regime of the overlay. In summary, the hardness results indicate that the SWF-GTAW process provides better uniformity and a lower risk of HAZ originated failures, although the CWF-GTAW and DWF-GTAW processes are simpler in terms of operation.

4. Conclusion

This study evaluated the performance of TIG welding processes with constant current and conventional wire feeding (CWF-GTAW), TIG with constant current and dynamic wire feeding (DWF-GTAW) and TIG with synchronized pulsed current and dynamic wire feeding (SWF-GTAW) for cladding steel pipes with Inconel 625 alloy. The optical emission spectroscopy tests revealed that the three processes showed similar levels of dilution, preserving the chemical composition of the deposited material. All processes proved viable for applications requiring high resistance to corrosion and wear, while maintaining the integrity of the filler material. Macrographic analysis showed homogeneity of the layer thickness (~1.5 mm) and metallurgical continuity between the overlays for the SWF-GTAW and DWF-GTAW processes, with no occurrence of defects such as cracks or lack of fusion. The SWF-GTAW process showed a slight superiority in terms of superficial uniformity.

The panoramic analyses indicated that the SWF-GTAW process showed possibly higher agitation of the molten metal. There was evidence of localized regions with higher iron contents in the overlay, which can decrease corrosion resistance in critical applications if close to the surface. On the other hand, the DWF-GTAW process showed a more homogeneous layer, suggesting better preservation of the properties of the cladded material. The CWF-GTAW process showed intermediate behavior, with good homogeneity, but slightly inferior to DWF-GTAW, especially in terms of layer thickness.

The microhardness analysis revealed that the CWF-GTAW process showed higher and more heterogeneous hardness values, with peaks over 400 HV in the HAZ, which may indicate local susceptibility to failure under severe operating conditions. The SWF-GTAW process, in contrast, showed a more controlled and homogeneous hardness profile, with smoother hardness gradients, favoring the integrity of the overlay. Meanwhile, the DWF-GTAW process showed less constant hardness behavior throughout the overlay regions, with marked variations.

Most of the results favor the synchronized current with dynamic feeding as the best option for this cladding operation. Despite being a more complex variant to implement and operate, SWF-GTAW shows great potential for developments and industrial applications.

References

- DA CUNHA, T. V., DOS SANTOS, F.J., VOIGT, A.L. (2022). Study on the influence of operational conditions on weld bead morphology produced through TIG process with longitudinal wire oscillation. J Braz Soc Mech Sci Eng 44(7):292. https://doi.org/10.1007/s40430-022-03582-z
- DUTRA, J. C. (2023). Ciência e Tecnologia da Soldagem a Arco Voltaico Dos Fundamentos às Modernas Técnicas. Editora Alfa Centauri Ltda.
- EWM. (2024, April 28). TigSpeed TIG cold/hot wire welding [Brochure] 2018. www.ewm-group.com
- Fronius. (2024, April 28). *Dynamic wire TIG cold wire welding [Brochure] 2022*. TIG-Dynamic Wire. https://www.fronius.com/en/welding-technology/product-information/iwave-tig-welding-system/tig-dynamicwire
- PAES, L. E. D. S. (2016). Soldagem TIG Orbital Técnica de Alimentação Dinâmica do Arame Visando Aumento na Produtividade (Master's thesis). Federal University of Santa Catarina, Santa Catarina, Brazil.
- PIGOZZO, I. O. (2024). Sobre a caracterização da transferência metálica no processo TIG com técnicas avançadas de alimentação de arame (Doctoral dissertation). Federal University of Santa Catarina, Santa Catarina, Brazil.
- PIGOZZO, I.O., SILVA, R.H.G.e., GALEAZZI, D., PEREIRA, A.S. (2022). Pulsed dynamic wire feeding with low insertion angle in GTAW process: a metal transfer characterization. Weld World 66(10):2107-2118. https://doi.org/10.1007/s40194-022-01352-y
- PIGOZZO, I.O., SILVA, R.H.G.E., VIVIANI, A.B. (2025). A novel monitoring and characterization approach of dynamic wire feeding in GTAW process. Weld World. https://doi.org/10.1007/s40194-025-01960-4
- RIFFEL, K.C., SILVA, R.H.G.E., HAUPT, W., DA SILVA, L.E., DALPIAZ, G. (2020). Effect of dynamic wire in the GTAW process: microstructure and corrosion resistance. J Mater Process Technol 285:116758. https://doi.org/10.1016/j.jmatprotec.2020.116758
- SILVA, R. G. N. (2016). Caracterização do Processo de Soldagem TIG com Alimentação de Arame Dinâmica em Alta Frequência 2016 (Undergraduate thesis). Federal University of Santa Catarina, Santa Catarina, Brazil.
- SILVA, R. H. G. E., SCHWEDERSK, M. B., ROSA, A. F. D. (2020). Evaluation of toptig technology applied to robotic orbital welding of 304L pipes. International Journal of Pressure Vessels and Piping, Volume 188, 202. DOI: https://doi.org/10.1016/j.ijpvp.2020.104229.
- TipTIG. (2024, April 28). *TipTIG The evolution of TIG welding [Brochure] 2016.* TIG-Dynamic Wire. www.tiptig-europe.eu
- TRINDADE, V. B., SOUZA, E. da S., PAULA, J. M. A. de, COSTA, M. C. M. de S., FARIA, G. L. de. (2017). Efeito de diferentes tratamentos térmicos sobre microestrutura e microdureza de um sistema aço C-Mn/revestimento de INCONEL 625. Tecnologia em Metalurgia e Mineração, v. 14, n.2, p. 167-174. DOI: http://dx.doi.org/10.4322/2176-1523.1182